Ecological Modelling 222 (2011) 2276–2290

Contents lists available at ScienceDirect

Ecological Modelling

journal homepage: www.elsevier.com/locate/ecolmodel

Modelling above- and below-ground mass loss and N dynamics in wooden dowels (LIDET) placed across North and Central America biomes at the decadal time scale

Amanda C. Smith[a], Jagtar S. Bhatti[b], Hua Chen[c], Mark E. Harmon[d], Paul A. Arp[a,*]

[a] Faculty of Forestry and Environmental Management, University of New Brunswick, 28 Dineen Drive, PO Box 44555, Fredericton, New Brunswick E3B 6C2, Canada
[b] Northern Forestry Centre, 5320 - 122nd Street, Edmonton, Alberta, T6H 3S5 Canada
[c] Biology Department,University of Illinois at Springfield, Springfield, IL 62703H, USA
[d] Department of Forest Ecosystems and Society, Oregon State University, Corvallis, OR 97331-5752, USA

ARTICLE INFO

Article history:
Received 5 March 2010
Received in revised form 1 September 2010
Accepted 14 September 2010
Available online 14 October 2010

Keywords:
Mass
Nitrogen
Wooden dowels
Tropical
Temperate
Boreal forests
Grasslands
Wetlands
Tundra

ABSTRACT

This article focuses on modelling above and below-ground mass loss and nitrogen (N) dynamics based on the wooden dowels (*Gonystylus bancanus* [Miq.] Kurz) of the decadal Long-term Intersite Decomposition Experiment (LIDET) data. These dowels were placed at 27 locations across North and Central America, involving tropical, temperate and boreal forests, grasslands, wetlands and the tundra. The dowel, inserted vertically into the soil with one half remaining exposed to the air, revealed fast mass and N losses under warm to humid conditions, and slow losses under wet as well as cold to dry conditions. The model formulation, referred to as the Wood Decomposition Model, or WDM, related these losses to (i) mean annual precipitation, mean monthly January and July air temperatures, and (ii) mean annual actual evapotranspiration (AET) at each location. The resulting calibrations conformed well to the time-in-field averages for mass remaining by location: R^2 = 0.83 and 0.90 for the lower and upper parts, respectively. These values dropped, respectively, to 0.41 and 0.55 for the N concentrations, and to 0.28 and 0.43 for N remaining. These reductions likely refer to error propagation and to as yet unresolved variations in N transference into and out of the wood specific to each individual dowel location. Recalibrating the model parameters by ecosystem type reduced the R^2 values for actual versus best-fitted mass loss by about 0.15. Doing the same without location- or ecosystem-specific adjustments reduced the R^2 values further, by about 0.3.
© 2010 Elsevier B.V. All rights reserved.

1. Introduction

Predicting the rate at which wood decays and mineralizes is important for assessing past, current and future ecosystem-level carbon (C) and nitrogen (N) responses under varying and changing climate conditions (Laiho and Prescott, 2004). Quantifying these processes, however, is a complex task because of their dependence on wood type, size, shape, density, lignin content, presence of wood preservatives, configuration of placement, wood-consuming organisms at work, and antecedent conditions (Harmon et al., 1995; Stevens, 1997). For example, woody debris that remains dry mineralizes fairly slowly. In contrast, wood that remains moist decays more quickly by providing optimal conditions for the entry and growth of decay-causing organisms such as fungi, bacteria, insects and wood dwellers. Wood placed into the ground may decay even more quickly than wood resting on the ground, depending on differences in moisture content and the physical, chemical and biological conditions of the adjacent soil (Busse, 1994; van der Wal et al., 2007). With regard to N, decaying wood has low N concentrations prior to decay (Hungate, 1940). Hence, transference of exogenous N from adjacent soil and decaying litter is likely to occur on account of physico-chemical processes such as diffusion from N-enriched soil solution into wood and biological processes such as N_2 fixation, and transfer of exogenous N and other nutrients into the wood via invading organisms, especially fungal mycelia (Becker, 1971; Ausmus, 1977; Freya et al., 2003). Ecologically, decaying wood may therefore provide temporary storage for N and other nutrients for later use (Boddy and Watkinson, 1995; Pyle and Brown, 1999).

To gain insight into the overall mass and N dynamics in decaying wood, recent forest litter studies dealing with forest litter decay across widely ranging site and climate conditions have also produced data for wood decay. Among these studies are: the Long-term Intersite Decomposition Experiment in the United States (LIDET, 1995; Parton et al., 2007; Adair et al., 2008), the Decomposition

* Corresponding author. Tel.: +1 506 453 4931; fax: +1 506 453 3538.
E-mail addresses: Jagtar.Bhatti@NRCan-RNCan.gc.ca (J.S. Bhatti), hchen40@uis.edu (H. Chen), Mark.Harmon@oregonstate.edu (M.E. Harmon), arp1@unb.ca, arp1@unb.ca (P.A. Arp).

0304-3800/$ – see front matter © 2010 Elsevier B.V. All rights reserved.
doi:10.1016/j.ecolmodel.2010.09.018

Study in Europe (DECO: Jansson and Reurslag, 1992), the Canadian Intersite Decomposition Experiment (CIDET: Trofymow and CIDET Working Group, 1998; Preston et al., 2009a,b) and the International Research Group on Wood Preservation (IRG, Jurgensen et al., 2003). In general, wood represents a large portion of annual forest litter accumulations on top or within the existing forest floor, and within the mineral soil in the form of decaying roots (Harmon et al., 1986; Scheu and Schauermann, 1994). Local forest disturbances due to, e.g., fire, insects, storms, harvesting and fires add to this accumulation in the form of snags, harvest residues, and whole-tree blow-down. Under moist and warm conditions, which are also associated with high rates of evapotranspiration, rates of wood decay and N gains and losses in fallen or soil-emplaced wood would be highest, and would be least under consistently cold and dry conditions (Griffith and Boddy, 1991; Meentemeyer, 1978; Currie et al., 2010). It is, however, not known to what extent wood decomposition and N uptake and losses influence one another, and how these rates vary above and below the ground within and across ecosystems from tropical to arctic biomes.

The objective of this article is to quantify and model the extent of above- and below-ground mass and N loss and N concentrations in the LIDET dowels over the course of a decade as affected by location, ecosystem type, and across locations using time-in-field and climate variables such as annual rates of actual evapotranspiration, precipitation, and mean monthly July and January temperature as predictor variables. The resulting model formulation followed the earlier work on the Forest Litter Decomposition Model FLDM by Zhang et al. (2007, 2008). This particular approach revealed that progressive mass losses and related changes in N content within decaying leaf litter can be modeled across boreal to temperate forest conditions for a wide range of leaf litters. This was done by using first- to second-order rate equations for leaf litter decay and N mineralization, and invoking a gradual transitioning from an initially fast and perhaps N limited decay process to slow and eventually C limited mass and N losses from the increasingly humified residue. A similar transitioning can be expected to occur in decaying wood.

2. Methods

2.1. LIDET procedures

Wooden dowels (61 cm long, 13 mm in diameter) of a tropical hardwood species *Gonystylus bancanus* [Miq.] Kurz, generally referred to as "ramin", were placed at 27 locations across North and Central America over the course of several years from 1990 to 1995 (LIDET, 1995). These locations represent a cross-section of biomes, varying from boreal, temperate and tropical forests to grasslands, wetlands and tundra (Table 1). Dowel emplacement occurred in two separate years in 24 locations, and only in one year at three locations. At each location, 48 dowels were placed on level ground

Table 1
LIDET locations, with specifications for mean annual precipitation, actual evapotranspiration (AET), and January and July temperatures, arranged by ecosystem type.

	Location	State/country	Ecosystem	17°5T Lat.	65°52' Long.	Elev. (m)	Ppt (cm)	AET (cm)	T_{Jan} (°C)	T_{Julv} (°C)
BNZ	Bonanza Creek Experimental Forest	Alalaska	Boreal Forest	64°45′	148°00′	300	40.3	36.0	−24.9	16.4
LVW	Loch Vale Watershed	Colorado	Boreal Forest	4O°1T	105°39′	3160	109.6	85.1	−9.3	14.6
JUN	Juneau	Alaska	Temperate Conifer Forest	58°00′	134°00′	100	287.8	49.5	−5.6	12.9
BSF	Blodgett State Research Forest	California	Temperate Conifer Forest	38°52	120°39′	1300	124.4	75.3	9.4	23.4
AND	H. J. Andrews Experimental Forest	Oregon	Temperate Conifer Forest	44°14′	122°11′	500	230.9	76.4	0.3	18.3
OLY	Olympic National Park	Washington	Temperate Conifer Forest	47°50′	122°53′	150	153.1	79.4	5.1	16.2
UFL	University of Florida	Florida	Temperate Conifer Forest	29°45′	82°30′	35	123.8	116.6	15.3	26.8
NLK	North Temp. Lakes (Trout Lake Station)	Wisconsin	Temperate Deciduous Forest	46°00′	89°40′	500	67.7	64.9	−12.5	19.1
HBR	Hubbard Brook Experimental Forest	New Hampshire	Temperate Deciduous Forest	43°56′	71°45′	300	139.6	71.2	−8.7	18.8
CDR	Cedar Creek Natural History Area	Minnesota	Temperate Woodland Humid Grassland	45°24′	93°12′	230	82.3	73.3	−13.5	21 2
HFR	Harvard Forest	Massachusetts	Temperate Deciduous Forest	42°40′	72°15′	335	115.2	85.1	−6.9	20
CWT	Coweeta Hydrol. Laboratory	North Carolina	Temperate Deciduous Forest	35°0′	85°30′	700	190.6	117.3	3	21.5
GSF	Guanica State Forest	Puerto Rico	Dry Tropical Forest	17°57′	65°52′	80	50.8	50.2	24.9	27.7
MTV	Monte Verde	Costa Rica	Tropical Elfin Cloud Forest	10°18′	84°48′	1550	268.5	108.4	18.3	16.8
LUQ	Luquillo Experimental Forest	Puerto Rico	Humid Tropical Forest	18°19′	65°49′	350	336.3	123.4	20.8	24.8
BCI	Barro Colorado Island	Panama	Humid Tropical Seasonal Forest	9°10′	79°51′	30	269.2	136.8	25.2	25.6
LBS	La Selva Biological Station	Costa Rica	Humid Tropical Forest	10°00′	83°00′	35	409.9	169.9	24.9	25.9
SMR	Santa Margarita Ecological Reserve	California	Annual Grassland	33°30′	117°45′	500	24.0	23.6	12	20
SEV	Sevilleta	New Mexico	Warm Semi-desert	34°29′	106°40′	1572	25.4	25.2	2.9	25
JRN	Jornada Experimental Range	New Mexico	Warm Semi-desert	32°30′	106°45′	1410	29.8	29.2	3.8	26
CPR	Central Plains Eperimental Range	Colorado	Temperate Shortgrass	40°49′	104°46′	1650	44.0	43.0	−3.1	21.6
KNZ	Konza Praerie Research	Kansas	Temperate Tallgrass	39°05′	93°35′	366	79.1	74.7	−2.7	26.6
KBS	Kellogg Biological Station	Michigan	Agro Ecosystem	42°24′	85°24′	288	81.1	70.6	−5.1	22.5
VCR	Virginia Coast Reserve	Virginia	Wetland	37°30′	75°40′	0	113.8	99.3	3.1	25
NIN	North Inlet (Hobcaw Barony)	South Carolina	Wetland	33°30′	79°13′	2	149.1	120.6	8.4	26.9
ARC	Arctic Site, Toolik Lake	Alaska	Tundra	68°38′	122°11′	760	32.7	28.4	−20.3	10.8
NWT	Niwot Ridge & Green Lakes Valley	Colorado	Tundra	40°03′	105°37′	3650	124.9	64.7	−13.2	8.2

Table 2
Number of years referring to dowel placement and retrieval, and total number of upper and lower dowel parts retrieved.

Location	Number of years with dowel retrieval following dowel placement					Total number of dowel parts retrieved	
	1990	1991	1992	1994	1995	Above-ground	Below-ground
BNZ	10	–	–	6	–	63	63
LVW	–	10	–	7	–	66	56
JUN	–	4	–	1	–	20	20
BSF	–	–	10	7	–	68	67
AND	10	–	–	6	–	61	53
OLY	7, 6	–	–	6	–	49	41
UFL	8, 5	–	–	5	–	45	32
NLK	2	–	–	–	–	8	8
HBR	6	–	–	2	–	31	28
CDR	8, 7	–	–	6	–	48	38
HFR	10, 9	–	–	6	–	63	54
CWT	10, 5	–	–	6, 5	–	48	34
GSF	–	10, 9	–	2	–	45	43
MTV	–	–	7, 6	1	–	28	23
LBS	9, 8	–	–	2	–	36	35
BCI	–	–	6	–	–	22	23
LUQ	10	–	–	–	–	40	38
SMR	8, 6	–	–	5	–	44	40
SEV	8	–	–	4	–	46	44
JRN	10	–	–	7	–	63	61
CPR	10	–	–	6	–	64	53
KNZ	9	–	–	5	–	55	48
KBS	2	–	–	5	–	28	28
VCR	–	7, 6	–	4	–	30	28
NIN	5	–	–	–	–	16	15
ARC	10	–	–	–	5	55	60
NWT	9	–	–	5	–	51	47
					Sum	1193	1080

1 m apart along a straight line, with four replicates available for potential retrieval for up to 10 years, depending on personnel and resources available at each location, and on decomposition progress towards irretrievability (Table 2). The lower half of each dowel was inserted into the ground, leaving the other half exposed to the air. The 1990, 1991 and 1992 dowels were placed into the ground without mesh wrapping (1 mm mesh size), while dowels placed in 1994 and 1995 were mesh-wrapped to enable a complete recovery of the decaying wood. Upon retrieval, dowels were analyzed for total mass remaining and N, ash and moisture content (Harmon and Sexton, 1996; Harmon et al., 1999). The resulting data were organized by dowel part (upper, lower), field emplacement year (5), location (27), time-in-field (up to 10 years), and replication (up to 4 per location and per retrieval year), yielding 2273 data combinations for statistical analysis.

2.2. Model formulation

It is hypothesized that the wooden dowels loose mass and gain as well as loose N according to the following FLDM-derived suggestion for a Wood Decomposition Model, or WDM:

$$\frac{dM}{dt} = -k_m(S) \cdot M \cdot \left[1 - \frac{[N]}{[N]_f}\left(1 - \frac{k_n(S)}{k_m(S)}\right)\right] \quad (1)$$

$$\frac{dN}{dt} = -k_n(S) \cdot N + k_a(S) \cdot \left(1 - \frac{[N]}{[N]_f}\right) \cdot M \quad (2)$$

where M and N are the total mass and N amounts remaining in the dowel, $[N] = N/M$ is the proportion or concentration of N in the dowel at any time (g of N per g of mass), and $[N]_f$ is the final N concentrations of the fully humified wood residue; $k_m(S)$, $k_n(S)$ and $k_a(S)$ are state-dependent functions to respectively evaluate the rate of mass loss and N transference out of and into the wood as affected by wood internal and external conditions. With this formulation, the rate of decay is assumed to be proportional to the amount of original mass remaining, and is limited by the extent to which [N] approaches its hypothesized final value $[N]_f$. The rate of N loss is assumed to be proportional to the current N content, modified by the N uptake rate, which is also proportional to the mass of wood, but modified by the $[N]/[N]_f$ ratio. The change in the N concentration within the decaying wood is consequently given by:

$$\frac{d[N]}{dt} = \{[N] \cdot [k_m(S) - k_n(S)] + k_a(S)]\} \left(1 - \frac{[N]}{[N]_f}\right) \quad (3)$$

which suggests that [N] increases, decreases or stays the same depending on the numerical values for [N], $k_m(S)$, $k_n(S)$ and $k_a(S)$. For example, the rate of mass loss is greater than rate of N loss when $k_m(S) > k_n(S)$ and $k_a(S) = 0$ (no exogenous uptake). For this case, [N] should increase gradually. Note that dM/dt is, at least initially, practically independent of [N] so that $dM/dt = -k_m(S)\, M$ as along as $[N] \ll [N]_f$. However, as t approaches infinity ($t \to \infty$), and in accordance with mathematical and ecological expectations and requirements:

1. dN/dM becomes equal to N/M which then becomes $[N]_f$;
2. both N and M approach 0;
3. N loss (1. term of Eq. (2)) and exogenous N uptake (2. term of Eq. (2)) approach 0.

Hence, wood decomposition would at first not be affected by the changing N concentrations within the decaying wood, as already reported by McClaugherty et al. (1985). Later on, and especially so at the humification stage, the gradual reduction of the readily metabolized C would have to become decay limiting, thereby leaving a gradually diminishing residue with a fixed and final N concentration.

In principle, the state-dependency of the $k_m(S)$, $k_n(S)$ and $k_a(S)$ parameters needs to reflect (i) the overall moisture (MC) and temperature (T) conditions of the air- and soil-exposed dowel parts at each location and (ii) other state-dependent factors such as microbial composition, soil acidity, and wood composition, especially

Table 3
Model formulation for the mass and N dynamics in the air- and soil-exposed portions of the LIDET dowels: definitions, values, and units, and data sources.

Symbol	Definition	Data source/values	Units	Eq(s).
M	Total mass remaining in the litter bag at time t	Data and model output	g	1
N	Nitrogen mass remaining at time t	Data and model output	g	2
[N]	Nitrogen concentration at time t	Data and model output	%	1, 2, 3, 7
f(MC,T)	Climate influence factor for litter decomposition and nitrogen mineralization	Model output		5, 6
ppt	Mean annual precipitation	Table 1	mm year^{-1}	5
PPt_0	Precicipation reference	1000	mm year^{-1}	5
T_{Jan}	Mean monthly January temperature	Table 1	°C	5
T_{July}	Mean monthly July temperature	Table 1	°C	5
T_{ref}	July reference temperature	15	°C	5
AET	Mean annual evapotranspiration	Table 1	mm year^{-1}	6
AET_{ref}	AET reference	162	mm year^{-1}	6
$[N]_f$	Final nitrogen concentration in well decomposed wood	2.4	%	2, 3
k_m,k_n	Parameters for mass loss and N mineralization from decaying wood	Table 4	year^{-1}	1, 2, 3, 7
k_n/k_m	Lumped parameter relating N mineralization to mass loss, based on Eq. (7)	Table 4		7
k_a	Parameter for exogenous N transference into wood	Table 4	year^{-1}	3
p_0	Parameter to adjust the T_{Jan} influence on f(MC, T) for the upper and lower dowel parts	Air-exposed: −1, Soil exposed: 1		5
Ea	Activation energy for wood decay	66,500 ± 2,900	J mol^{-1}	5
R	Universal gas constant	8.31	J mol^{-1} °C^{-1}	5

referring to the acid-unhydrolyzable fraction. Due to lack of site- and wood-specific information, using data made from one type of wood only, on and assuming that k_m(S), k_n(S) and k_a(S) are affected by changing moisture and temperature conditions in the same way, one sets:

$$k_m(S) = k_m f(MC, T),\ k_n(S) = k_n f(MC, T),\ \text{and}$$
$$k_a(S) = k_a f(MC, T) \quad (4)$$

with f(MC,T) as the moisture- and temperature-dependent part of k_m(S), k_n(S) and k_a(S) functions, and it is assumed that k_m and k_n (the mineralization coefficients for mass and N), and k_a (the uptake coefficient for exogenous N) would be independent of the moisture and temperature conditions within the wood. Assuming further that changes in moisture and temperature affect the overall decay process independently of one another is equivalent to setting f(MC,T) = f(MC) f(T). Since the actual moisture and temperature conditions within the LIDET dowels are unknown, f(MC,T) was formulated as follows (Zhang et al., 2007):

$$f(MC, T) = \left(\frac{ppt}{ppt_{ref}}\right)^{0.5} \left[1 + p_0 \quad \min\left(0, \frac{T_{Jan}}{abs(T_{July} - T_{Jan})}\right)\right] exp\left[-\frac{Ea}{R}\left(\frac{1}{T_{July}} - \frac{1}{T_{ref}}\right)\right] \quad (5)$$

where the annual precipitation rate (ppt, in mm) and mean monthly air temperatures for July (T_{July}) and January (T_{Jan}) serve as surrogates to capture the effect of wood moisture and temperature on the annual mass and N changes within the upper and lower dowel parts. For sub-zero temperature conditions, setting $p_0 = -1$ for the upper dowel part is intended to reflect: (i) wood abrasion under wind-exposed arctic to subarctic conditions and other wind-exposed locations (Sonesson and Callaghan, 1991; Held et al., 2006; McKenna Neuman, 1993) and (ii) snow-ecological effects on wood decomposition and related net N loss (Jones and Pomeroy, 1999). In contrast, setting $p_0 = 1$ for the lower dowel part reflects the general lack of biological activity when the ground is frozen. The mean July air temperature serves as a surrogate for the temperature above and below the ground. Ea represents the activation energy of the wood decay process, and R is the universal gas constant (=8.31 J mol^{-1} C^{-1}). The ppt_{ref} and T_{ref} entries serve as reference values or scale coefficients for precipitation and temperature, set at 1000 mm year^{-1} and 15 °C, respectively. Hence, f(MC, T) = 1 when ppt = 1000 mm a^{-1}, T_{Jan} = 0 °C, and T_{July} = 15 °C. The exponent of 0.5 for ppt/ppt_{ref} reflects declining increases in wood decay with increasing ppt above ppt_{ref}. An alternative formulation for f(MC,T) sets (Meentemeyer, 1978; McClaugherty et al., 1985; Currie et al., 2010):

$$f(MC, T) = \frac{AET}{AET_{ref}} \quad (6)$$

where AET is the mean annual actual evapotranspiration rate at each LIDET location, and AET_{ref} is a reference value so that Eqs. (5) and (6) produce similar k_m values.

Generally, wood decay is portrayed as a first-order reaction process, involving one or two wood compartments: a decay resistant component, and a component that is less resistant (Hale and Pastor, 1998; Romero et al., 2005). The above formulation, however, is a single-compartment formulation, but accounts for a gradual, non-exponential slow-down by making the decomposition rate dependent on the difference between the current and finally attainable N concentration within the decaying wood. At the same time, the rate of N loss and potential exogenous N uptake is linked to the rate of mass loss as well. To emphasize the overall state-dependency of the above formulation, it is instructive to relate the changes in N content and mass to the changing N concentrations within the dowels, i.e.:

$$\frac{dN}{dM} = \frac{k_n}{k_m} \frac{1 + (k_a/k_n)((1/[N]) - (1/[N]_f))}{1 - (1 - k_n/k_m)([N]/[N]_f)}[N] \quad (7)$$

with k_n/k_m and k_a/k_n as lumped parameters, and [N] as the only variable needed to relate changes in N to changes in M. For a summary of WDM definitions, parameters, and data sources, see Table 3.

2.3. Computational methods

The quality of the compiled data was checked by plotting one variable with another, to locate and remove inconsistencies, outliers and non-feasible data entries. The original weight, ash and moisture content determinations and the determinations of M% and N% remaining assisted in this process. Faulty data entries were located and removed. These generally arose from analyzing insufficient or soil-contaminated samples. Averaging the filtered data for the above- and below-ground dowel parts by time-in-field and by location produced 224 data combinations by location and year of data retrieval, including initial dowel mass and N content.

ModelMaker software (ModelMaker, 1999) was used to calibrate the above formulation with the time-in-field averages for M and N remaining and for [N] at each location, by dowel part. This was done with the built-in Marquardt least-squares non-linear

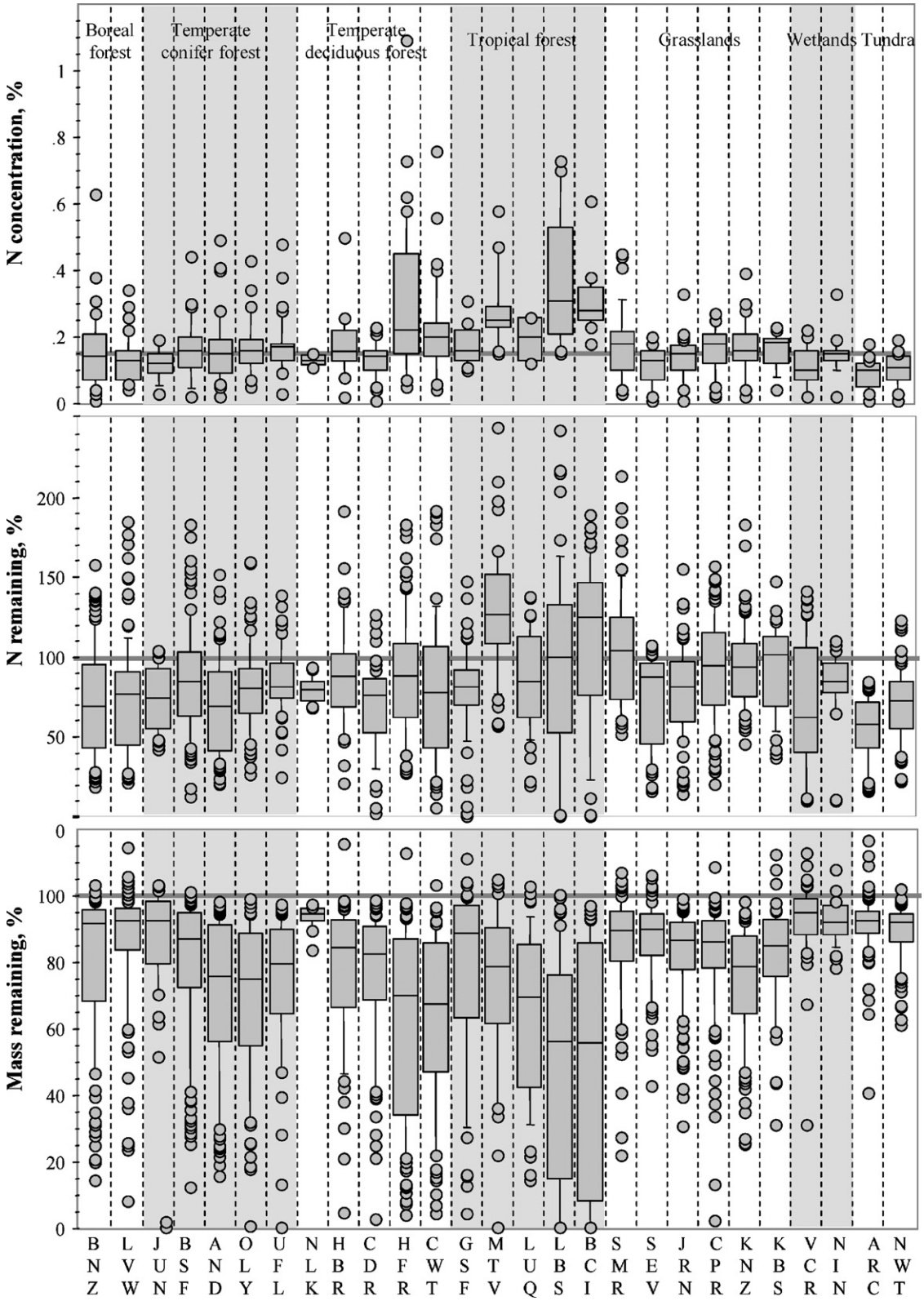

Fig. 1. Box-and-whisker plots for the mass and N remaining and N concentration data in dowels placed at 27 LIDET locations across North America (Table 1), collected over a period of up to 10 years at each location. Shown are the 10, 25, 50, 75, and 90th percentiles of the original data including outliers (dots). Locations are arranged by ecosystem type from left to right: forests (boreal, temperate conifer, temperate deciduous, tropical), grasslands, wetlands, tundra.

regression routine, used for minimizing the residuals between the actual and calibrated values, and for generating the least-squares estimate for k_m, k_n/k_m, k_a, Ea, and $[N]_f$. The mean annual entries for ppt, T_{Jan} and T_{Jul} or AET for each LIDET location in Table 1 served as model input for Eqs. (5) and (6). The best-fitted location-specific k_m values were then compared with the best-fitted k_m values for each ecosystem type, and for all locations combined. Because of the high variability of the N data and related convergence issues

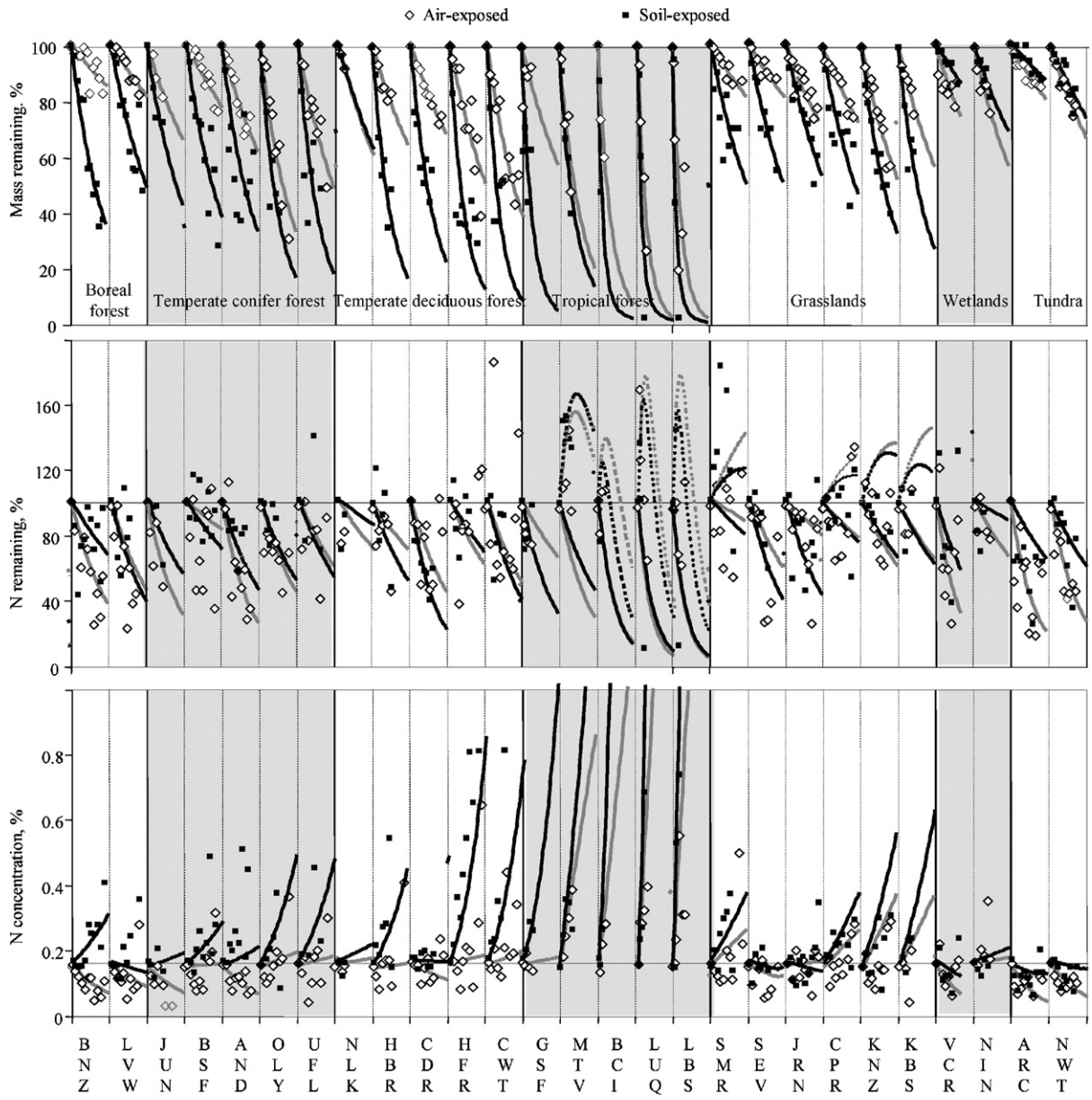

Fig. 2. Time series plots for modeled (lines, Tables 3 and 5 specifications) and actual time-in-field averages for mass and N remaining and N concentrations, all in %, for the upper (open dots) and soil-exposed (filled dots) dowel parts at each LIDET location, with all locations lined up along the *x*-axis based on the Table 1 pattern, with each slot representing a 0–12 year interval. The solid and shaded lines represent the model calculation assuming no exogenous N uptake everywhere ($k_a = 0$). The dashed solid and shaded lines are restricted to those locations with significant exogenous uptake patterns, i.e., MTV, BCI, LUQ, LBS, SMR, CPR, KNZ, and KBS.

in deriving best-fitted k_n and k_a parameters for some of the locations, it was decided to derive a common k_n/k_m value for each of the upper and lower dowel parts for all locations. This common value was then adjusted with location-specific multipliers to improve the general conformance between the N loss and N concentration data and the corresponding model output, as needed. For the k_a parameter, it was decided to use $k_a = 0$ as default value for dowel parts with no appreciable or consistent N gains after field placement. For dowel parts with appreciable N gains, it was decided to derive a single common value for both dowel parts for all such locations, and to adjust this value with a location-specific multiplier for the upper or lower dowel parts as needed. The Ea and $[N]_f$ entries were held in common for all locations and both dowel parts. Convergence towards an unambiguous $[N]_f$ value was not achievable. This parameter was therefore held constant at $[N]_f = 0.024$ (Table 3), which is about double the highest value among the [N] data, and is equivalent to a final C/N ratio of about 20. Overall model output and best-fitted parameter values were fairly insensitive towards increasing or decreasing this number by a factor of about 2. To balance the simultaneous minimization of the residuals between the calibrated actual mass and N data, it was necessary to convert the N concentrations from percent (%) to per thousand (‰).

3. Results

An overview of the data for the remaining mass and N as well as the N concentrations and variations associated with each of the retrieved LIDET dowels is presented in Fig. 1 by way of box-and-whisker plots by ecosystem type. These plots were grouped, from left to right, by ecosystem type from forests (boreal, temperate coniferous, temperate deciduous, and tropical), to grasslands, wetlands and tundra, and were also arranged within each ecosystem type from low to high AET. On display are the 10th, 25th, 50th,

Table 4
Multiple regression results for predicting the mass and N loss (%) of the lower dowel parts from the upper dowel parts; uML refers to the annual time-in-field averages for the mass from the upper dowel parts, grouped by ecosystem type; uNL refers to the corresponding N losses, not grouped by ecosystem type.

	Variable	Coefficient	SE	*t*-Value	*p*-Value
Mass loss (%)	Intercept	5.79	1.17	5.0	<0.0001
	uML, grasslands	0.49	0.14	3.6	0.0004
$R^2 = 0.82$ RMSE = 9.5	uML, boreal forest	1.36	0.33	4.2	<0.0001
	uML, coniferous forest	1.07	0.13	8.4	<0.0001
	uML, deciduous forest	1.31	0.13	10.1	<0.0001
	uML, tropical forest	1.27	0.09	14.7	<0.0001
	uML, tundra	−0.88	0.21	−4.3	<0.0001
	uML, wetlands	−0.56	0.21	−2.7	0.0075
	Time-in-field (years)	3.32	0.39	8.5	<0.0001
N loss (%)$R^2 = 0.22$RMSE = 23.7	All locations, uNL(%)	1.76	0.11	16.2	<0.0001

70th and 90th percentiles of the data for each location, and all outliers below the 10th and above the 90th percentiles. As shown, mass losses increased fairly quickly, especially at moist and warm locations. In contrast, the N remaining pattern was highly variable, and in excess of 100% at four of the five tropical forest locations (MTV, BCI, LUQ, LBS), and at four of the six grassland locations (KBS, KNZ, CPR, SMR). The opposite occurred at the two tundra locations (ARC, NWT), the two boreal locations (BNZ, LVW), the two temperate conifer locations (AND, JUN), and one grassland location (SEV), where N remaining stayed below the initial value.

Re-plotting the data following averaging the time-in-field replicates at each location across the 1990, 1992, 1994 and 1995 placement years in Fig. 2 led to the following observations:

1. Mass loss from the upper dowel parts generally increased with increasing moisture and temperature conditions except when too wet, and were lowest at the arctic (ARC) and boreal locations (BNZ, LVW), and highest at the tropical locations (BCI, LUQ, LBS). For the grassland locations, mass loss would increase in direct proportion with increasing precipitation and actual evapo-transpiration, being lowest at SMR, and highest at KNZ.
2. Mass losses generally occurred faster from the lower than the upper dowel parts, except at the arctic (ARC, NWT) and wetland (VCR, NIN) locations where the opposite occurred. These differences were therefore affected by ecosystem type, and also increased with increasing time-in-field, as indicated by the multiple regression results listed in Table 4. Altogether, these results and the scatter plot of the actual versus best-fitted data in Fig. 3 suggest that the average mass losses from the lower dowel parts can be predicted from the average mass losses of the upper dowel parts at $R^2 = 0.71$ with a root mean square error of RMSE = ±7%.
3. The averaged N content within the upper and lower dowel parts were quite variable, but indicated that the lower dowel parts conserved N better than the upper dowel parts, i.e., N loss (lower parts) = 0.56 N loss (upper parts, see Table 4). This correlation was not affected by ecosystem type, as shown in Fig. 3 (bottom).
4. The N losses were not correlated with the mass losses, neither for the upper ($R^2 = 0.0013$) nor for the lower dowel parts ($R^2 = 0.022$).

Calibrating the k_m, k_n and k_a parameters in three ways, namely by location, by ecosystem type, and keeping all three parameters in common across all locations led to the compilation in Table 5 and the following results:

1. The best-fitted location-specific k_m values varied by ecosystem type, with fairly consistent trends by ecosystem type, but not

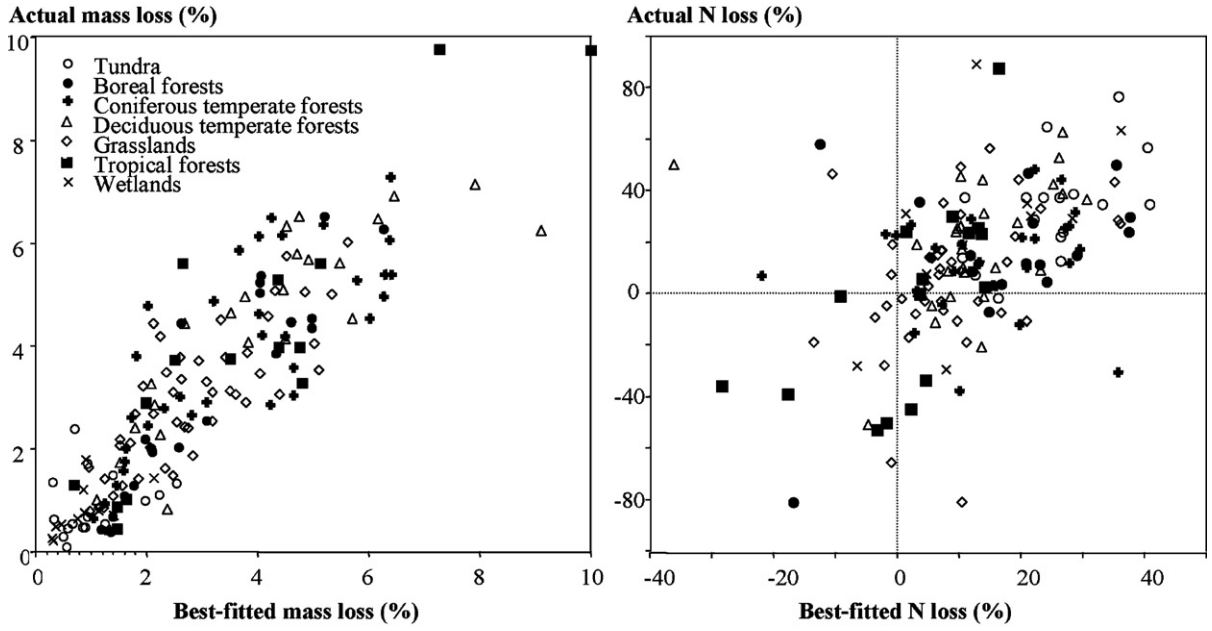

Fig. 3. Actual versus best-fitted mass (top) and N (bottom) losses in bottom dowel parts, using the mass and N loss data from the upper dowel parts as predictor variables, showing that the resulting mass loss predictions for the lower dowel parts would depend on ecosystem type, but the corresponding N loss predictions would not.

Table 5
Best-fitted k_m values (a^{-1}) by location, by ecosystem type, and held in common across all locations, together with best-fitted common k_n/k_m and k_a (a^{-1}) values, and their multipliers for all locations. Also shown are the standard errors of estimate for (i) the common k_m, k_n/k_m and k_a value, and the k_m values by ecosystem type.

Ecosystem	Location	Location-calibrated k_m				k_m by ecosystem, with standard error of estimate[a]				k_n/k_m multiplier		k_a multiplier	
		Air		Soil		Air		Soil		Air	Soil	Air	Soil
		Eq. (5)	Eq. (6)	Eq. (5)	Eq. (6)	Eq. (5)	Eq. (6)	Eq. (5)	Eq. (6)				
Boreal Forest	BNZ	0.010	0.016	0.343	0.138	**0.011**	**0.009**	**0.167**	**0.048**	10	1	0	0
	LVW	0.012	0.010	0.107	0.039	*0.003*	*0.003*	*0.017*	*0.004*	6	4	0	0
Temperate	JUN	0.020	0.037	0.079	0.077	**0.018**	**0.022**	**0.057**	**0.059**	4	2	0	0
Conifer Forest	BSF	0.009	0.015	0.036	0.059	*0.002*	*0.002*	*0.004*	*0.004*	1	1	0	0
	AND	0.019	0.026	0.048	0.065					4	2	0	0
	OLY	0.069	0.060	0.121	0.106					1	1	0	0
	UFL	0.019	0.027	0.049	0.070					1	1	0	0
Temperate	NLK	0.024	0.025	0.058	0.028	**0.026**	**0.026**	**0.109**	**0.081**	1	1	0	0
Deciduous	HBR	0.017	0.027	0.141	0.116	*0.002*	*0.002*	*0.008*	*0.005*	1	1	0	0
Forest	CDR	0.015	0.023	0.129	0.088					3	3	0	0
	HFR	0.028	0.026	0.162	0.123					1	0.5	0	0
	CWT	0.033	0.036	0.094	0.104					1	1	0	0
Tropical Forest	GSF	0.042	0.049	0.124	0.289	**0.060**	**0.072**	**0.121**	**0.140**	1	1	0	0
	MTV	0.071	0.064	0.100	0.090	*0.006*	*0.006*	*0.010*	*0.012*	1	1	3	10
	LUQ	0.072	0.136	0.134	0.251					1	1	1	1
	BCI	0.054	0.069	0.121	0.154					1	1	1	1
	LBS	0.058	0.097	0.120	0.200					1	1	1	1
Grasslands	SMR	0.023	0.039	0.082	0.138	**0.020**	**0.030**	**0.051**	**0.071**	1	1	1	1
	SEV	0.013	0.034	0.049	0.126	*0.002*	*0.003*	*0.004*	*0.004*	4	4	0	0
	JRN	0.019	0.050	0.036	0.096					1	4	0	0
	CPR	0.020	0.033	0.064	0.081					1	1	1	3
	KNZ	0.020	0.039	0.044	0.070					1	1	1	3
	KBS	0.023	0.035	0.080	0.086					1	1	1	1
Wetlands	VCR	0.014	0.020	0.007	0.010	**0.013**	**0.015**	**0.008**	**0.009**	6	12	0	0
	NIN	0.014	0.022	0.009	0.015	*0.008*	*0.003*	*0.003*	*0.003*	1	1	0	0
Tundra	ARC	0.026	0.028	0.089	0.021	**0.031**	**0.017**	**0.113**	**0.021**	12	10	0	0
	NWT	0.033	0.024	0.118	0.020	*0.007*	*0.004*	*0.032*	*0.004*	5	5	0	0
Common across all locations[b]		0.022	0.025	0.062	0.056					"Common" k_n/k_m value[c]		"Common" k_a value[d]	
±Standard error of estimate		0.001	0.002	0.003	0.002					0.85 ± 0.04	0.35 ± 0.02	0.0188 ± 0.0030	

[a] Averages by ecosystem bold, coefficients of variation *italic*.
[b] Averages and coefficients of variation across ecosystems weighted by number of locations per ecosystem type.
[c] Common k_n/k_m, value: computed for all locations, assuming $k_a = 0$.
[d] Ccommon k_a value: for locations with k_a multipliers >0 only.

across the forest locations. In detail, (i) OLY displayed considerably higher k_m values for the upper and lower dowel parts than the other temperate forest locations; (ii) BSF had a low k_m value for the upper dowel part; (iv) BNZ had exceptionally high k_m values for the lower dowel parts; (iv) NLK had fairly low k_m values for the lower dowel part compared to the other deciduous forest locations.

2. The common k_m values across all locations were quite similar by dowel part: for the upper dowel parts, k_m (Eq. (5)) = 0.022 ± 0.001 and k_m (Eq. (6)) = 0.025 ± 0.001); for the lower dowel parts, k_m (Eq. (5)) = 0.056 ± 0.002 and k_m (Eq. (6)) = 0.062 ± 0.003 (Table 5, bottom left).
3. Due to the high variability of the data for N remaining and for the N concentrations in the wooden dowels, least-squares convergence toward best-fitted k_n/k_m and k_a values were not consistently obtainable by location or by ecosystem type. There was, however, convergence towards a common k_n/k_m value for all locations, and a common k_a value for the eight locations with N remaining > 100%. Inspecting the resulting plots for N remaining and N concentration versus time-in-field suggested that location-specific k_n/k_m adjustments were needed. These adjustments led to $k_n/k_m > 1$ (i.e., N losses occurred faster than mass losses) for (i) the upper dowel parts at BNZ, LVW, JUN, AND, SEV, VCR, ARC and NWT, and (ii) the lower dowel parts at LVW, SEV, JRN, VCR, AER and NWT. Several of these locations have cold and/or dry climate conditions. The main exceptions were VCR, CDR, and AND. At HFR, N retention in the lower dowel part was particularly pronounced. For $k_a > 0$, multiplier values other than 1 were needed for the lower dowel parts at one tropical location (MTV) and two grassland locations (CPR and KNZ).
4. The best-fitted results for M, N and [N] using Eq. (5) for the f(MC,T) formulation are presented in Fig. 2 in the form of the 10-year plots for the upper (shaded lines) and lower (solid lines) dowel parts at each location. These lines correspond quite well with the dots that represent the time-in-field averages for M, N and [N] at each location.
5. Fig. 2 shows two additional lines (dashed) for the MTV, BCI, LUQ, LBS, KBS, KNZ, CPR, SMR locations with apparent exogenous N uptake. These lines imply immediate and steady increases in N content and concentrations following dowel placement at all these locations. Thereafter, N content would slow down for the grasslands and start to decrease fairly rapidly at the BCI, LUQ, LBS and MTV tropical forest locations. According to Eq. (3), k_n/k_m and k_a multiplier adjustments were needed for these locations as well. The resulting changes, however, remained small for most cases because [N] remained $\ll [N]_f$.

The goodness-of-fit achieved by location is portrayed in Fig. 4 by plotting the actual- versus best-fitted values for the mass and N losses, and for [N]. These plots show a fairly even scatter for the mass and N remaining plots, and a fairly clustered plot for the N concentrations about the initial N concentration of 0.15%. The R^2 values associated with these plots were as follows:

$$\text{Mass loss}\ \ (R^2 = 0.87) \gg [\text{N}]\,(R^2 = 0.42) > \text{N loss}\ \ (R^2 = 0.40)$$

for the upper dowel parts, and

$$\text{Mass loss}\ \ (R^2 = 0.76) \gg [\text{N}](R^2 = 0.55) \gg \text{N loss}\ \ (R^2 = 0.29)$$

for the lower dowel parts. These sequences were, in part, affected by error propagation, because the unaccounted variations for M remaining limited the extent to which [N] could be calibrated, since "modeled [N]" = "modeled N"/"modeled M". In turn, the unaccounted variations for M and [N] contributed both to the N remaining variations, because:

$$\text{N}_{\text{remaining}} = \frac{M[\text{N}]}{M_0[\text{N}]_0},$$

where M_0 and $[\text{N}]_0$ are the initial M and [N] values.

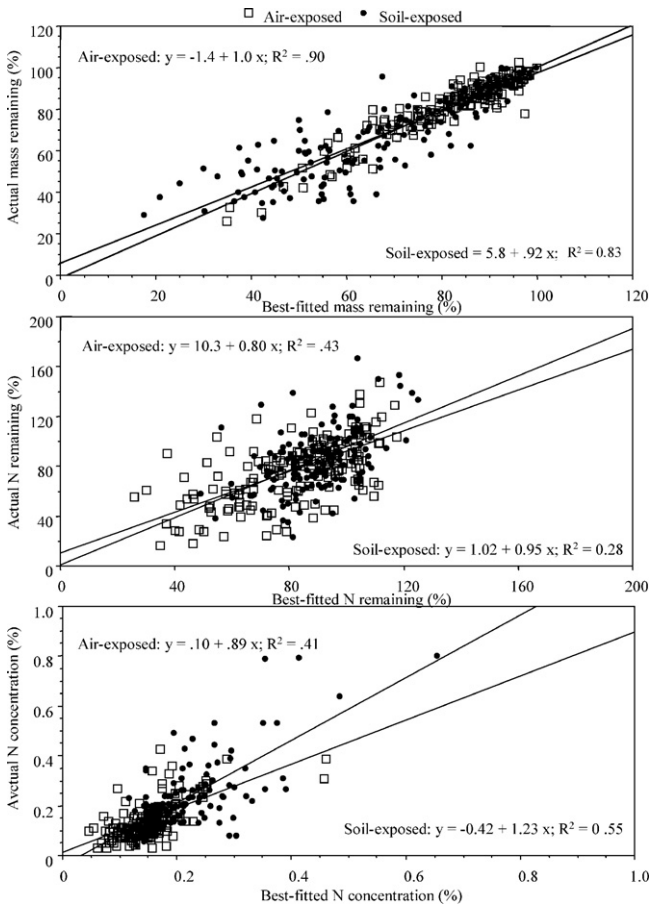

Fig. 4. Scatter plots of actual versus model-calibrated values (averaged by location) for mass and N remaining, and N concentrations in the upper (open dots) and lower (filled dots) parts of the LIDET dowels, together with best-fitted regression lines (climate formulation based on Eq. (5); parameters are specified in Table 5).

Combining the best-fitted k_m and k_n/k_m values with the climate-affected f(MC,T) estimates via Eq. (5) based on the Table 1 specifications for p_0, ppt_{ref} and T_{ref} produced the location-specific plots for the climate-adjusted $k_m(S)$ and $k_n(S)$ rate of decay and N loss parameters in Fig. 5. These were arranged by increasing AET values from left to right, by ecosystem type.

In detail, these plots indicate that the $k_m(S)$ values remained higher for the lower than the upper dowel parts, with these differences generally increasing from the wetlands to the two tundra locations and from there to the grasslands, the boreal and temperate conifer forests, and the temperate deciduous and tropical forests, with the tropical cloud forest at MTV being an exception. In comparison to the $k_m(S)$ pattern, $k_n(S)$ was less well defined across the ecosystem types. Highest $k_n(S)$ values were associated with the humid tropical forest locations BCI, LUQ and LBS. The $k_n(S)$ values of upper dowel parts at the two tundra locations and the VCR wetland location were also fairly high. The lowest $k_n(S)$ values occurred (i) within the lower dowel parts at the NIN wetland location and at the NLK forest location, and (ii) within the upper dowel parts at the BSF forest location and the SMR, JRN and CPR grassland locations.

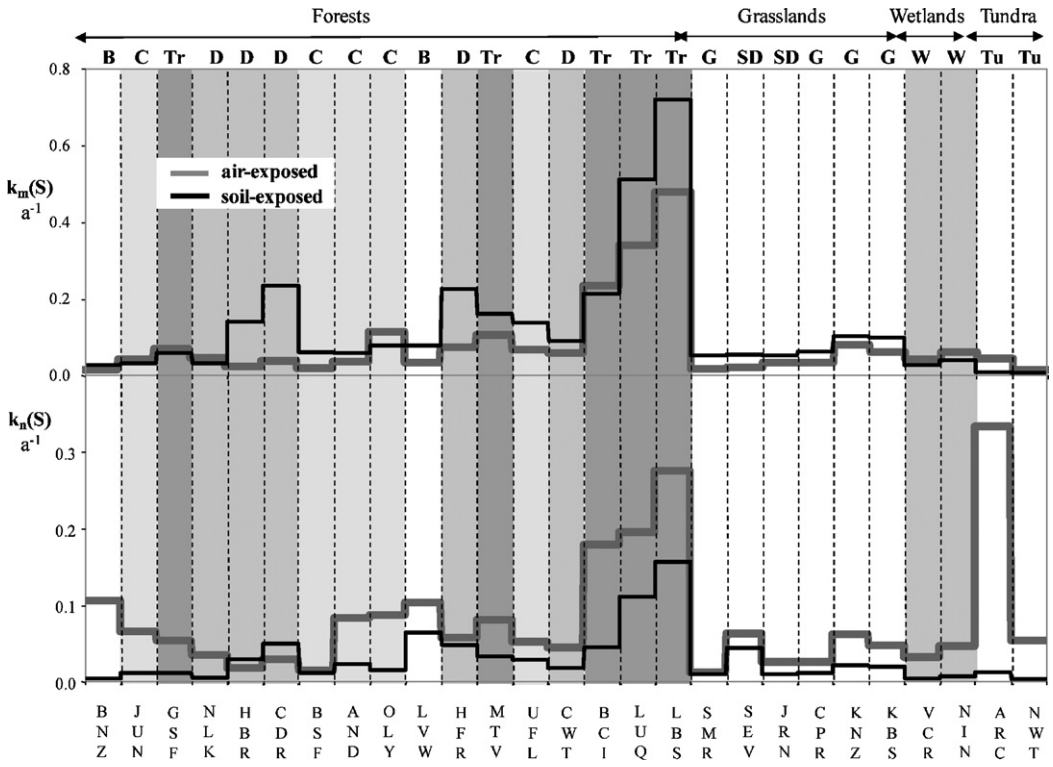

Fig. 5. Plots for the best-fitted mass and N loss coefficients $k_m(S) = k_m$ f(MC,T) and $k_n(S) = k_n$ f(MC,T) for the air- and soil-exposed dowel parts at each LIDET location, with f(MC,T) based on the Eq. (5) calculations. Abbreviations: B: boreal forest; C conifer forest, D deciduous forest, G grassland, SD semi-desert, Tr tropical forest, Tu tundra, W wetland.

Re-calibrating the model for mass remaining with the time-in-field averaged mass loss data for the upper and lower dowel parts simultaneously (i) across all 27 locations, (ii) by ecosystem type, and finally (iii) without location and ecosystem type adjustments yielded the following R^2 sequences for mass remaining, respectively:

0.84, 0.64, and 0.32 with Eq. (5), using the ppt and T_{Jan} and T_{July} estimates for each location;
0.84, 0.71, and 0.42 with Eq. (6), using the annual estimates for AET for each location

(details not shown). This suggests that employing Eq. (6) would statistically be more robust than employing Eq. (5) for generalized model applications. However, using Eq. (5) has the advantage of (i) directly projecting mass and N loss from annual precipitation and monthly temperature specifications, and (ii) automatically accounting for the influence of sub-zero temperatures ($T < 0\,^{\circ}C$) on annual mass and N losses from wood.Examining the time-in-field averages for the mass and N losses by location and year-of-dowel placement yielded no significant differences by year-of-dowel placement. In addition, there were no significant mass and N loss differences between the dowels that were mesh-wrapped or not.

4. Discussion

The mass and N loss dynamics within the decaying LIDET dowels appear to be similar to the reported mass and N loss dynamics in LIDET leaf litter bags (Parton et al., 2007). However, only one mass compartment and one N compartment were needed for quantifying the overall mass and N losses from decaying wood by location and by ecosystem type. In contrast, at least three mass and two N compartments were needed to quantify mass and N losses from litter bags at about the same R^2 level (Adair et al., 2008; Zhang et al., 2008). The likely reason for this is that ramin wood is chemically and physiologically less complex than leaf litter, and may as such offer less varying resistance towards slow but complete or nearly complete decay. This is underscored by the low initial N concentration of 0.15%, which is less than the range of initial 0.38–2% N concentration range for leaf litter (Adair et al., 2008), and is considerably less than the $[N]_f$ value for fully humified organic matter. According to the above model formulation and results, ramin wood therefore tracks the exponential decay pattern much longer towards final decomposition than leaf litter. In comparison to the above 0.007–0.289 a^{-1} single-compartment k_m range for wood decay, best-fitted k_m values for leaf litter varied from about 8 to 0.4 and 0.1 a^{-1} for the fast, slow and very slow leaf litter compartments, respectively (Zhang et al., 2007, 2008).

The time-in-field averaged data for mass and N loss and for the N concentrations were best modeled by way of location-specific calibrations. Re-calibrating the model by determining the ecosystem-specific values for k_m but retaining the location-specific k_n and k_a values and associated multipliers caused a small drop in goodness-of-fit, from $R^2 = 0.84$ to 0.71 (using Eq. (6)). Re-calibrating once again by forcing the above- and below-ground k_m values to be common across all locations caused a large drop in R^2 from 0.71 to 0.42. This drop was directly related to locations with exceptionally high or low k_m values per ecosystem type, i.e.: (i) the high k_m values for the lower dowel part at BNZ (boreal forest), (ii) the low k_m values for the lower dowel part at LVW (boreal forest), NLK (temperate deciduous forest) and MTV (tropical cloud forest), (iii) the high k_m values for both dowel parts at OLY (temperate conifer rain forest), and (iv) the low k_m values for the upper dowel parts at BSF (temperate conifer forest) and GSF (dry tropical forest). The low k_m values for the upper dowel parts at BSF and GSF were likely due to fairly dry near-ground conditions at these conifer sites, especially during the growing season when most of the incoming precipitation would be lost again through canopy interception and evapotranspiration

(Schaap et al., 1997). In contrast, forests in humid areas would maintain high moisture conditions at and near the ground because of low below- to above-canopy air exchange, thereby encouraging wood decay, thus resulting in high k_m values, as noted for the coastal rain forest at OLY, and for the humid tropical forests at BCI, LBS and LUQ. As such, the rate of wood decay, and of forest litter decay in general, should vary with stand structure, i.e., would decrease with increasing canopy openings, as reported by Takyu et al. (2003), Kurzatkowski et al. (2004), Martius et al. (2004a,b), Sariyildiz (2008), and Toledo et al. (2009). Examining the k_m entries in Table 5 in this regard revealed that the standard deviations of these values were, on average by ecosystem type, about 5 and 2 times more variable for the upper and lower dowel parts across the forested than the open-field locations, respectively (lower dowel parts at BNZ and LVW excluded).

Some of the k_m variations in Table 5 would also be due to local variations in soil moisture and temperature as affected by location (microclimate), soil drainage and soil depth. For example, Jurgensen et al. (2006) examined wood strength and mass loss from southern pine (*Pinus* spp.) stakes placed along a gradient of Scots pine plantations on well-drained coarse-textured soils from northern Finland to southern Poland. These stakes were 33 cm long and were placed vertically into well-drained coarse-textured soils, and flush to the mineral soil surface underneath the organic forest floor mat. The results showed that: (i) wood strength loss was directly relatable to mass loss; (ii) wood strength and mass loss increased from north to south, but were more closely related to the variations in annual air temperature than precipitation (mean annual temperature range: −1 to 7 °C; ppt range: 450–760 mm a^{-1}; ppt = 471 + 24.3 T_{annual}, R^2 = 0.48); (iii) these losses decreased from the top to the bottom third of the stakes. The last trend is consistent with generally advanced wood decay in soil-anchored wooden poles and stakes just below the soil surface. The authors attributed this trend to decreasing soil temperatures with increasing soil depth. Such a change, however, would be quite small summer through winter within the top 30 cm of heat-conductive soils (Balland and Arp, 2005). Moisture levels within the stakes would, however, vary strongly from top to bottom due to frequent rewetting at and near the soil surface, and due to generally dry conditions at the bottom on account of persistent water uptake from the root-permeated soils throughout summer to early fall. In this way, extensive root-induced moisture uptake may have contributed to the low k_m value at the NLK location. This low value could, however, also be an artifact on account of the low data coverage for NLK (Table 2).

Wood decay would be slow in poorly to very poorly drained soils such as those at NIN and VCR, and as reported by Moore et al. (2005) for several boreal to subarctic upland-wetland locations in Canada, using wooden blocks (*Tsuga heterophylla*) placed on the ground and buried 30 cm into the soil (CIDET protocol, Trofymow, 1998). Wood buried in areas with cryosolic soils would also decay very slowly, as was the case at ARC and NWT. This may have been the case for the BNZ location in the interior of Alaska as well, but the fairly productive white spruce stand at this dowel location implied fairly warm and moist soil conditions during the growing season, and these decay-promoting conditions would have giving rise to the high k_m values for the lower dowel parts at BNZ.

By and within ecosystem type and for each location, additional and perhaps as yet unaccounted decay variations would be due to differences in type, activities and availabilities of wood decay organisms, depending on, e.g., the proximity of the wooden pieces and debris to areas with high concentrations of wood consumers (Genet et al., 2001; Kurzatkowski et al., 2004; Martius et al., 2004a,b; Moorhead and Sinsabaugh, 2006). For example, González et al. (2008) noticed that mass losses from flat-lying aspen stakes were higher under dry than humid tropical forest locations, presumably due to variations in termite activity. The presence and activities of wood consumers would also depend on local soil conditions, as these vary strongly over the range of short distances. For example, mound-and-pit microtopography in forest soils would lead to more acidifying and humifying forest litter in pits than on mounds, with the former mostly subject to extensive fungal decay while the latter providing a better substrate for wood-consuming bacteriae and insects (Robertson, 1987; Reich et al., 1997; Venterea et al., 2003; Schultz and Nicholas, 2010).

Relating wood decay to actual moisture and temperature conditions within the upper and lower dowel parts by season or month and perhaps even by day should, in principle, improve the constancy of the k_m values within and across ecosystem locations and climate zones. Progress in this direction was made by Adair et al. (2008), using f(MC,*T*) formulations similar to Eq. (5) to capture the monthly progress of time-in-field averaged mass losses from root and leaf litter bags across the LIDET locations, with best-fitted results without location- or ecosystem-specific adjustments producing an R^2 value of 0.68. Further improvements in this regard could be made by reformulating Eq. (5) with modeled or actual wood or soil moisture and temperature data. For example, Brischke and Rapp (2008) monitored the effect of daily changing moisture and temperature conditions in air-exposed wood [Scots pine sapwood (*Pinus sylvestris*) and Douglas fir heartwood (*Pseudotsuga menziesii*)] on structural wood decay (mechanical wood failure) over the course of 7 years at 23 European field locations. They then correlated wood failure – rated as 0 (sound), 1 (slight attack), 2 (moderate attack), 3 (severe attack) or 4 (failure) – to a daily f(MC,T) dose function. Through least-squares fitting, they concluded that their f(MC,T) formulation led to a feasible basis for predicting the wood service life at R^2 = 0.94 for Scots pine. A corresponding function was not generated from the Douglas fir heartwood data on account of reduced moisture entry into this wood and, hence, low to no decay.

The prevailing climate and vegetation-soil conditions would also influence the extent of N retention and transferences into and out of the LIDET dowels above and below the ground. This was demonstrated by the weak but nevertheless significant N loss correlation between the upper and lower dowel parts (Fig. 3). The typically higher N concentrations within the lower dowel parts (i) would generally be caused by faster wood consumption, (ii) would be better sheltered against wetting and drying and freezing and thawing, and (iii) early N losses would in part be compensated by exogenous N uptake. In contrast to the mass loss correlation between the upper and lower dowel parts, this correlation was not significantly affected by ecosystem type. The higher N loss rates from the upper dowel parts would, at least to some of extent, be due to an initially fairly mobile N content in the form of, e.g., amino acids (Nordin et al., 2001) and other nutrients (Terziev and Nilsson, 1999). If so, then wood desiccation (King et al., 1974) coupled with physical abrasion (Sonesson and Callaghan, 1991) would assist in lowering the N content from the upper dowel parts, especially so at the tundra locations and other dry areas, such as the semi-desert locations at JRN and SEV, and the boreal forest locations at BNZ and LVW. In general, the best-fitted "common" k_n/k_m value of 0.85 for the upper dowel parts was considerably higher than the corresponding value of 0.35 for the lower dowel parts. Hence, the lower dowel parts were more N conservative than the upper dowel parts, thus leading to higher N concentrations (or decreasing C/N ratios) within the buried wood over time, as also reported by Boddy and Watkinson (1995), Torres (1994), Holub et al. (2001), Laiho and Prescott (2004), Jurgensen et al. (2006), and Sarjubala Devi and Yadava (2007).

The extent to which exogenous N is taken up appears to depend on a continuous replenishment of externally available N, including N_2 fixation. For example, Melillo et al. (1983) reported that placing

wood in the form of wood chips derived from alder (*Alnus rugosa*), paper birch (*Betula papyrifera*), trembling aspen (*Populus tremuloides*), balsam fir (*Abies balsamea*), and black spruce (*Picea mariana*) directly into streams increased the N concentrations within the stream-placed wood rather dramatically, from up to about 200% (alder) to 1200% (black spruce), and in direct proportion with the lignin content of the wood. Romero et al. (2005) reported increased N retention in *Laguncularia racemosa*, *Avicennia germinan* and *Rhizophora* wood placed above and below the ground within a mangrove forest. Some of these increases would be due to biofilm formations within and on water submerged structures (Eggert and Wallace, 2007). Such increases, however, did not occur systematically within the upper and soil-exposed ramin wood across the LIDET locations. Here, exogenous N uptake was generally restricted to some of the dowels placed at the humid tropical forest locations (BCI, LBS, LUQ, MTV), and was very sporadic at the grassland locations (the semi-desert locations at SEV and JRN excluded), possibly on account of uneven grazing and related N mobilization and re-absorption of ammonia by wood within and above the soil (Bariska and Popper, 1975; Frank and Evans, 1997). Boulanger and Sirois (2006) reported no significant increases in the N content of post-fire coarse woody debris of black spruce (*Picea mariana*) logs and snags over the course of 30 years. Fahey et al. (1991) reported only modest N increases in post-harvest Sitka spruce wood residues. In contrast, Jurgensen et al. (2006) reported N gains up to about 300% in pine stakes three years after soil placement, in direct proportion with increasing mass loss. This was undoubtedly due to the very low initial N concentration of about 0.033% within these stakes, and in general conformance to the WDM formulation. In this regard, N_2 fixation does not take part in the early stage of wood decomposition, but follows the build-up of fungal biomass which facilitates the gradual entry and activities of N_2-fixing bacteria at a later wood decomposition stage (Larsen et al., 1978; Spano et al., 1982; Jurgensen et al., 1984; Hendrickson, 1991; Hicks et al., 2003).

van der Wal et al. (2007) reported that nutrient additions to soil next to surface-placed and buried birch sawdust and wooden blocks increased the overall decay process, but on upland soils only. N-accelerated mass loss, however, was not evident for the upper or lower dowel parts at LIDET locations with $k_a > 0$ and elsewhere. This is consistent with the Eq. (1) implied slowdown of mass loss with increasing [N]. This slowdown, however, would be small as long as $[N] \ll [N]_f$. A N-induced slow-down in mass loss was in fact observed for decaying leaf litter from Western hemlock (*Tsuga heterophylla*), Western red cedar (*Thuja plicata*) and Douglas-fir following sewage sludge treatments, but the same did not occur (i.e., no effect) in N-fertilized leaf litter from Paper birch (*Betula papyrifera*), Jack pine (*Pinus banksiana*) and Lodgepole pine (*Pinus contorta*) (Prescott, 1995). The general trend of low or no N-induced effects on forest litter decay has been reviewed and analyzed by Prescott et al. (2004) and Prescott (2005, 2010).

Some of the location-specific differences in wood decay and N net mineralization may be related to topographic effects and antecedent site conditions, as noted for old-growth versus second-growth forest stands (Fisk et al., 2002). In another example, mass loss from ramin dowels placed into the soil of an annually burned and unburned tallgrass prairie was faster on shallow upland and slope sites than on deeper lowland sites. The accompanying N concentrations were unaffected by topographic position (O'Lear et al., 1996). Here, the N-limiting conditions of the grassland soils likely contributed to the lack of net exogenous N transfer from the soil into the wood. O'Lear et al. (1996) also found that soil-placed dowels showed higher mass loss and N concentrations in dowels placed on annually burnt sites than in the dowels placed on un-burnt or occasionally burnt sites. This was attributed to fire-induced differences in soil microflora. The moisture and temperature conditions were noted to be the same for the burned and unburned plots.

In reference to wooden pieces other than dowels, there would be further complications, as detailed, e.g., for oak logs by Schowalter et al. (1998) by year, and for roots and twigs by Scheu and Schauermann (1994) by months. Wood type also matters, as discussed by Syafii et al. (1988), Schowalter et al. (1998), Harmon et al. (2000), and Laiho and Prescott (2004). To accommodate these complications, it would be necessary to re-evaluate k_m, k_n and k_a by type and location, as done for leaf litter decay by Zhang et al. (2007). In general, wood decay would generally decrease with increasing N (Eq. (1)) and acid-unhydrolyzable (AUR) content within the wood (Harmon et al., 2000; Adair et al., 2008), with the latter related to wood type by species if not trait, and additional variations arising from pith and heartwood to sapwood and periderm (Weedon et al., 2009). In analogy to the FLDM formulation for forest litter decomposition, one could generalize the above results by setting:

$$k_{m,\text{wood type}} = k_{m,\text{ramin}} \left(\frac{\text{AUR}_{\text{ramin}}}{\text{AUR}_{\text{wood type}}} \right)^a$$

and

$$\left(\frac{k_n}{k_m} \right)_{\text{wood type}} = \left(\frac{k_n}{k_m} \right)_{\text{ramin}} \left(\frac{[N]_{\text{ramin}}}{[N]_{\text{wood type}}} \right)^b$$

where AUR and N refer to the initial AUR and N concentrations, and a and b are adjustable parameters, with 1 being the default value. In this regard, Jurgensen et al. (2003) reported that mass losses from the AUR (lignin), cellulose and hemicellulose fractions in soil-buried southern pine stakes did not differ significantly from one another following three years of soil placement. Similarly placed aspen stakes, however, incurred higher cellulose than lignin losses over the course of 3 years.

Converting the k_m and k_n/k_m values and their multipliers in Table 5 to $k_m(S)$ and $k_n(S)$ using Eq. (5) produced the plots in Fig. 5 to show how the actual rate coefficients for mass and N loss from the upper and lower dowel parts vary across the LIDET locations and by ecosystem type. These plots were organized by increasing AET from left to right, by ecosystem type (forests, grasslands, wetlands, tundra). From this, it can be concluded (i) that $k_m(S)$ and $k_n(S)$ follow the pattern of the local climate variables in general, (ii) that the $k_m(S)$ values for the upper and lower dowel parts were closely associated with one another, (iii) that the latter exceeded the former except on the wetlands and on the tundra, and (iv) that there were considerable $k_n(S)$ differences for the upper and lower dowel parts such that the latter exceeded the former in almost all cases, with HBR and CRD being the exceptions and the other temperate deciduous having fairly similar values for both dowel parts. The $k_m(S)$ values so generated tend to be in good agreement with the 0.0025–0.07 a^{-1} rate of decay coefficients reported by Laiho and Prescott (2004) for coarse woody debris in northern coniferous forests. There is also a good match with (i) the 0.06–0.11 a^{-1} $k_m(S)$ values for standing dead and fallen sugar maple logs at a deciduous location in Tenessee, USA (Onega and Eickmeier, 1991), and (ii) the wood turn-over rate of 0.11 a^{-1} for the mostly deciduous trees at Hubbard Brook (New Hampshire, USA; Fahey et al., 2005). For dry tropical conditions on Yucatan, Harmon and Chen (1991) determined $k_m(S)$-equivalent values ranging from 0.15 to 1.02 a^{-1} for fine woody debris, and from 0.008 to 0.615 a^{-1} for coarse woody debris. The estimated $k_m(S)$ values for wood at the Luquillo Experimental Forest, Puerto Rico (LUQ, several species) were similar, and varied from 0.29 to 0.69 a^{-1} along stream, riparian and upslope areas (Vogt et al., 1996).

The plots in Fig. 6 provide an overview summary of the best-fitted $k_m(S)$ and $k_n(S)$ values (Eq. (6)) by location (dots) and by ecosystem type (polygons) in relation to the Table 1 entry for mean annual AET. The extent of conformance and con-conformance to the general wood decay and N mineralization expectation with increas-

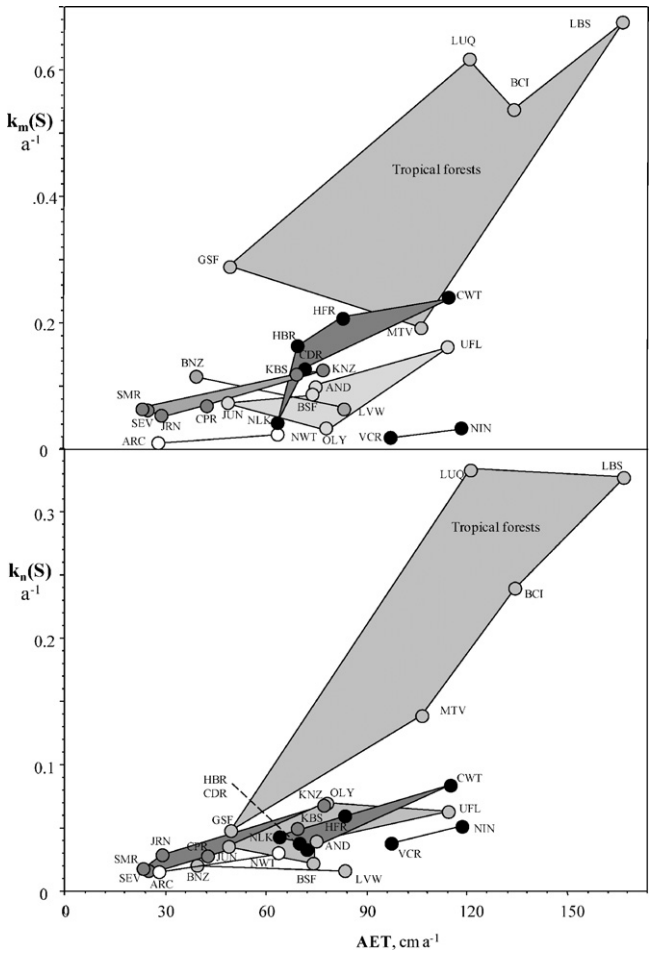

Fig. 6. Plot of $k_m(S)$ and $k_n(S)$ values versus AET, by location (dots) and ecosystem type (polygons).

ing mean annual AET is reflected by the orientation and shape of the polygons. This conformance increases with increased polygon elongation along the 1:1 line, while the width of these polygons reflects the extent that the wood decay and N mineralization rates cannot be captured by mean annual AET specifications alone. Since the polygons for the tropical forests are the largest and least narrow, this means that there are greater uncertainties in relating wood decay and N mineralization in topical forest biomes to simple climate indicators than what appears to be the case for the other biomes of this study.

Note that all of the above asserts that wood decay is essentially subject to hydrothermal controls (Griffith and Boddy, 1991). This would, however, not necessarily be the case for each individual dowel location and especially not so in terms of exogenous N uptake and retention, but such details appear to become less important through the time-in-field averaging process across the dowel spots per location, and by averaging across the locations per ecosystem type as well.

5. Concluding remarks

Examining the mass and N loss data within the upper and lower dowel parts across the 27 North American LIDET locations in the context of the above model formulation for wood decay and associated N dynamics revealed a number of patterns for the time-in-field averaged values, namely:

1. Up to about 83–90% of the below- and above-ground mass loss variations could be captured based on the location-specific k_m calibrations in Table 5, and using local data for (i) mean annual precipitation, mean monthly January and July temperatures (Eq. (5)) and (ii) mean annual evapotranspiration (Eq. (6)). These numbers drop, respectively, to 70–74% by way of ecosystem- instead of location-specific parameter calibrations, and to 34% and 43% by calibrating across all locations without location or ecosystem adjustments.
2. The mass loss variations associated with the lower dowel parts could be related to the mass loss variations associated with the upper dowel parts at $R^2 = 0.82$, using ecosystem type and time-in-field as additional regression variables (Table 4).
3. The N losses from the lower dowel parts were also correlated with the N losses from the upper dowel parts, but this correlation was essentially independent of ecosystem type and time-in-field.
4. The soil-exposed dowel parts lost mass about twice as fast as the upper parts; in contrast, the latter lost N twice as fast as the upper parts. About 40% of the N loss and 55% of the N concentration variations could be accounted for by way of location-specific k_n and k_a parameter adjustments, following outlier removal.
5. Exogenous N uptake was noted to occur at certain locations, but that was generally sporadic and likely specific to each dowel location, especially on the grassland locations other than the semi-desert locations. The observed N dynamics for the wooden dowels therefore differed from the corresponding leaf litter dynamics, with the latter accommodating exogenous N in a systematic relationship with varying N concentrations within the decaying leaf litter (Eq. (7); Zhang et al., 2008).

Further work is required (i) to discern the dependence of the k_m, k_n (or k_n/k_m) and k_a (or k_a/k_n) parameters by location and wood-type variations, (ii) to examine how other factors such as extent of canopy cover, wood placement, soil depth, and shape and type of wood also influence the overall decay dynamics, and (iii) to determine how to extrapolate the parameterization results gleaned from dowels towards projecting the decay and N dynamics in coarse woody debris involving stemwood, bark, branches, twigs, and roots. Yet another challenge is to generalize the results of this study to the forecasting of biomass, C and N dynamics from arctic to tropical conditions, and from the uplands to the wetlands within these systems (Boulanger and Sirois, 2006). Adding compartments such as acid-hydrolyzable and non-hyrolyzable fractions, microbial biomass, ash content, and build-up of humified residues would allow quantifying wood decay in further detail. For more detailed analyses, one would need seasonal or monthly data as well. In summary, the results suggest that the WDM formulation provides a useful framework for quantifying average end-of-year mass and N remaining in upper and soil-exposed wood placed across a wide range of location, ecosystem and climate conditions for at least 10 years if not longer.

Acknowledgements

This study would not have been possible without the dedicated effort of many people associated with the LIDET project, to collect and process samples, and to provide background information on site characteristics and climate. This study was supported by grants from the US National Science Foundation (DEB-9108329, DEB-9806493) in addition to numerous grants and in-kind assistance at each location. The analysis and modelling component of this article was supported by an NSERC Discovery Grant to PAA, by the NSERC-sponsored Sustainable Forest Management Network, and by the Forest Watershed Research Centre at UNB, as part of

developing tools and rules for forest biomass harvesting in New Brunswick, Nova Scotia and elsewhere.

References

Adair, E.C., Parton, W.J., Del Grosso, S.J., Silver, W.L., Harmon, M.E., Hall, S.A., Burke, I.C., Hart, S.C., 2008. A simple three pool model accurately describes patterns of (LIDET) data set. Global Change Biol. 114, 2636–2660.

Ausmus, B.S., 1977. Regulation of wood decomposition rates by arthropod and annelid populations. Soil organisms as components of ecosystems. Ecol. Bull. (Stockholm) 25, 180–192.

Balland, V., Arp, P.A., 2005. Modeling soil thermal conductivities over a wide range of conditions. J. Eng. Env. Sci. 4, 549–558.

Bariska, M., Popper, R., 1975. Ammonia sorption isotherms of wood and cotton cellulose. Wood Sci. Technol. 9, 153–163.

Becker, G., 1971. Physiological influences on wood-destroying insects of wood compounds and substances produced by microorganisms. Wood Sci. Technol. 5, 236–246.

Boddy, L., Watkinson, S.C., 1995. Wood decomposition, higher fungi, and their role in nutrient redistribution. Can. J. Bot. 73, 1377–1383.

Boulanger, Y., Sirois, L., 2006. Postfire dynamics of black spruce coarse woody debris in northern boreal forest of Quebec. Can. J. For. Res. 36, 1770–1780.

Brischke, C., Rapp, A.O., 2008. Dose-response relationships between wood moisture content, wood temperature and fungal decay determined for 23 European field test sites. Wood Sci. Technol., doi:10.1007/s00226-008-0191-8.

Busse, M.D., 1994. Downed bole-wood decomposition in Lodgepole Pine forests of Central Oregon. Soil Sci. Soc. Am. J. 58, 221–227.

Currie, W.S., Harmon, M.E., Burke, I.C., Hart, S.C., Parton, W.J., 2010. Cross-biome transplants of plant litter show decomposition models extend to a broader climatic range but lose predictability at the decadal time scale. Global Change Biol. 16, 1744–1761.

Eggert, S.L., Wallace, G.B., 2007. Wood biofilm as a food resource for stream detritivores. Limnol. Oceanogr. 52, 1239–1245.

Fahey, T.J., Stevens, P.A., Hornung, M., Rowland, P., 1991. Decomposition and nutrient release from logging residue following conventional harvest of Sitka spruce in North Wales. Forestry 64, 289–301.

Fahey, T.J., Siccama, T.G., Driscoll, C.T., Likens, G.E., Campbell, J., Johnson, C.E., Battles, J.J., Aber, J.D., Cole, J.J., Fisk, M.C., Groffman, P.M., Hamburg, S.P., Holmes, R.T., Schwarz, P.A., Yanai, R.D., 2005. The biogeochemistry of carbon at Hubbard Brook. Biogeochemistry 75, 109–176.

Fisk, M.C., Zak, D.R., Crow, T.R., 2002. Nitrogen storage and cycling in old- and second-growth northern hardwood forests. Ecology 83, 73–87.

Frank, D.A., Evans, R.D., 1997. Effects of native grazers on grassland n cycling in Yellowstone National Park. Ecology 78, 2238–2248.

Freya, S.D., Six, J., Elliott, E.T., 2003. Reciprocal transfer of carbon and nitrogen by decomposer fungi at the soil-litter interface. Soil Biol. Biochem. 35, 1001–1004.

Genet, J.A., Genet, K.S., Burton, T.M., Murphy, P.G., Lugo, A.E., 2001. Response of termite community and wood decomposition rates to habitat fragmentation in a subtropical dry forest. Trop. Ecol. 42, 35–49.

González, G., Gould, W.A., Hudak, A.T., Nettleton Hollingsworth, T., 2008. Decay of aspen (*Populus tremuloides* Michx.) wood in moist and dry boreal, temperate, and tropical forest fragments. Ambio 37, 588–597.

Griffith, G.S., Boddy, L., 1991. Fungal decomposition of attached angiosperm twigs: III. Effect of water potential and temperature on fungal growth, survival and decay of wood. New Phytol. 117, 259–269.

Hale, C., Pastor, J., 1998. Nitrogen content, decay rates, and decompositional dynamics of hollow versus solid hardwood logs in hardwood forests of Minnesota, U.S.A. Can. J. For. Res. 28, 1276–1285.

Harmon, M.E., Chen, H., 1991. Coarse woody debris dynamics in two old-growth ecosystems. BioSci. 41, 604–610.

Harmon, M.E., Franklin, J.F., Swanson, F.J., Sollins, P., Gregory, S.V., Lattin, J.D., Anderson, N.H., Cline, S.P., Aumen, N.G., Sedell, J.R., Lienkaemper, G.W., Cro-mack K.Jr., Cummins, K.W., 1986. Ecology of coarse woody debris in temperate ecosystems. Adv. Ecol. Res. 15, 133–302.

Harmon, M.E., Whigham, D.F., Sexton, J., Olmsted, I., 1995. Decomposition and mass of woody detritus in the dry tropical forests of the Northeastern Yucatan Peninsula, Mexico. Biotropica 27, 305–316.

Harmon M.E., Sexton J. Guidelines for measurements of woody detritus in forest ecosystems. Publication No. 20. U.S. LTER Network Office, University of Washington, Seattle; 1996.

Harmon, M.E, Nadelhoffer, K.N., Blair, J.M., 1999. Measuring decomposition, nutrient turnover, and stores in plant litter. In: Robertson, G.P., Coleman, D.C., Bledsoe, C.S., Sollins, P. (Eds.), Standard soil methods for long-germ ecological research. Oxford University Press, New York, pp. 202–240.

Harmon, M.E., Krankina, O.N., Sexton, J., 2000. Decomposition vectors: a new approach to estimating woody detritus decomposition dynamics. Can. J. For. Res. 30, 76–84.

Held, B.W., Jurgens, J.A., Duncan, S.M., Farrell, R.L., Blanchette, R.A., 2006. Assessment of fungal diversity and deterioration in a wooden structure at New Harbor, Antarctica. Polar Biol. 29, 526–531.

Hendrickson, O.Q., 1991. Abundance and activity of N_2-fixing bacteria in decaying wood. Can. J. For. Res. 21, 1299–1304.

Holub, S.M., Spears, J.D.H., Lajtha, K., 2001. A reanalysis of nutrient dynamics in coniferous coarse woody debris. Can. J. For. Res. 31, 1894–1901.

Hicks, W.T., Harmon, M.E., Myrold, D.D., 2003. Biotic controls of nitrogen fixation and respiration in woody debris in the Pacific Northwest. For. Ecol. Manage. 176, 25–35.

Hungate, R.E., 1940. Nitrogen content of sound and decayed coniferous woods and its relation during decay. Bot. Gaz. 102, 382–392.

Jansson, P.-E., Reurslag, A., 1992. Climatic influence on litter decomposition: methods and some results of a NW-European transect. In: Teller, A., Mathy, P., Jeffers, J.N.R. (Eds.), Responses of Forest Ecosystems to Environmental Changes. pp. 351–358. Proceedings of First European Symposium on Terrestrial Ecosystems. Florence May 20–24, 1991, Commission of the European Communities. Elsevier Applied Science, London.

Jones, H.G., Pomeroy, J.W., 1999. The ecology of snow-covered systems: summary and relevance to Wolf Creek, Yukon. In: Pomeroy, J., Granger, R. (Eds.), Wolf Creek Research Basin: Hydrology, Ecology, Environment. National Water Research Institute, Minister of Environment, Saskatoon, pp. 1–14.

Jurgensen, M.F., Larsen, M.J., Spano, S.D., Harvey, A.E., Gale, M.R., 1984. Nitrogen fixation associated with increased wood decay in Douglas-fir residue. For. Sci. 30, 1038–1044.

King, B., Oxley, T.A., Long, K.D., 1974. Soluble nitrogen in wood and its redistribution on drying. Mater. Org. 9, 241–254.

Jurgensen, M., Reed, D., Page-Dumroese, D., Laks, P., Collins, A., Mroz, G., Degórski, M., 2006. Wood strength loss as a measure of decomposition in northern forest mineral soil. Eur. J. Soil Biol. 42, 23–31.

Jurgensen, M., Laks, P., Reed, D., Collins, A., Page-Dumroese, D., Crawford, D. Chemical, physical, and biological factors affecting wood decomposition in forest soils. *The International Research Group on Wood Preservation*. Paper prepared for the 34th Annual Meeting, Brisbane, Australia. IRG Secretariat SE-100 44 Stockholm, Sweden. IRG/WP 03-20281.

Kurzatkowski, D., Martius, C., Höfer, H., Garcia, M., Förster, B., Beck, L., Vlek, P., 2004. Litter decomposition, microbial biomass and activity of soil organisms in three agroforestry sites in Central Amazonia. Nutr. Cycl. Agroecosyst. 69, 257–267.

Laiho, R., Prescott, C.E., 2004. Decay and nutrient dynamics of coarse woody debris in northern coniferous forests: a synthesis. Can. J. For. Res. 34, 763–777.

Larsen, M.J., Jurgensen, M.F., Harvey, A.F., 1978. N_2 fixation associated with wood decayed by some common fungi in western Montana. Can. J. For. Res. 8, 341–345.

LIDET, 1995. Meeting the challenges of long-term, broad-scale ecological experiments. Report No. 19. US LTER Network Office, Seattle.

Martius, C., Höfer, H., Garcia, M.V.B., Römbke, J., Hanagarth, W., 2004a. Litter fall, litter stocks and decomposition rates in rainforest and agroforestry sites in central Amazonia. Nutr. Cycl. Agroecosyst. 68, 137–154.

Martius, C., Höfer, H., Garcia, M.V.B., Römbke, J., Förster, B., Hanagarth, W., 2004b. Microclimate in agroforestry systems in Central Amazonia: does canopy closure matter to soil organisms? Agroforest. Syst. 60, 291–304.

McClaugherty, C.A., Pastor, J., Aber, J.D., 1985. Forest litter decomposition in relation to soil nitrogen dynamics and litter quality. Ecology 66, 266–275.

McKenna Neuman, C.V., 1993. A review of aeolian transport processes in cold environments. Prog. Phys. Geogr. 17, 137–155.

Melillo, J.M., Naiman, R.J., Abet, J.D., Eshleman, K.N., 1983. The influence of substrate quality and stream size on wood decomposition dynamics. Oecologia (Berlin) 58, 281–285.

Meentemeyer, V., 1978. Macroclimate and lignin control of litter decomposition rates. Ecology 59, 465–472.

ModelMaker, 1999. Cherwell Scientific Ltd, Oxford, UK.

Moore, T.R., Trofymow, J.A., Siltanen, M., Prescott, C., CIDET Working Group, 2005. Patterns of decomposition and carbon, nitrogen, and phosphorus dynamics of litter in upland forest and peatland sites in central Canada. Can. J. For. Res. 35, 133–142.

Moorhead, D.L., Sinsabaugh, R.L., 2006. A theoretical model of litter decay and microbial interaction. Ecol. Monogr. 76, 151–174.

Nordin, A., Uggla, C., Nasholm, T., 2001. Nitrogen forms in bark, wood and foliage of nitrogen-fertilized *Pinus sylvestris*. Tree Physiol. 21, 59–64.

O'Lear, H.A., Seastedt, T.R., Briggs, J.M., Blair, J.M., Ramundo, R.A., 1996. Fire and topographic effects on decomposition rates and N dynamics of buried wood in tallgrass prairie. Soil Biol. Biochem. 28, 323–329.

Onega, T.L., Eickmeier, W.G., 1991. Woody detritus inputs and decomposition kinetics in a southern temperate deciduous forest. Bull. Torrey Bot. Club 118, 52–57.

Parton, W., Silver, W.L., Burke, I.C., Grassens, L., Harmon, M.E., Currie, W.S., King, J.Y., Adair, E.C., Brandt, L.A., Hart, S.C., Fasth, B., 2007. Global-scale similarities in nitrogen release patterns during long-term decomposition. Science 315, 361–364.

Prescott, C.E., 1995. Does nitrogen availability control rates of litter decomposition in forests. Plant Soil 169, 83–88.

Prescott, C.E., 2005. Do rates of litter decomposition tell us anything we really need to know? For. Ecol. Manage. 220, 66–74.

Prescott, C.E., 2010. Litter decomposition: what controls it and how can we alter it to sequester more carbon in forest soils? Biogeochemistry, doi:10.1007/s10533-010-9439-0.

Prescott, C.E., Blevins, L.L., Staley, C., 2004. Litter decomposition in British Columbia forests: controlling factors and influences of forestry activities. BCJ Ecosyst. Manage. 5, 44–57.

Preston, C.M., Nault, J.R., Trofymow, J.A., Smyth, C., CIDET Working Group, 2009a. Chemical changes during 6 years of decomposition of 11 litters in some Canadian forest sites. Part 1. Elemental composition, tannins, phenolics, and proximate fractions. Ecosystems 12, 1053–1077.

Preston, C.M., Nault, J.R., Trofymow, J.A., 2009b. Chemical changes during 6 years of decomposition of 11 litters in some Canadian forest sites. Part 1. ^{13}C abundance,

solid-State ^{13}C NMR spectroscopy and the meaning of "lignin". Ecosystems 12, 1078–1102.
Pyle, C., Brown, M.M., 1999. Heterogeneity of wood decay classes within hardwood. For. Ecol. Manage. 114, 253–259.
Reich, P.B., Grigal, D.F., Aber, J.D., Gower, S.T., 1997. Nitrogen mineralization and productivity in 50 hardwood and conifer stands on diverse soils. Ecology 78, 335–347.
Robertson, G.P., 1987. Nitrification in forested ecosystems. Philos. Trans. R. Soc. Lond. Ser. B, Biol. Sci. 296, 445–457.
Romero, L.M., Smith III, T.J., Fourqurean, J.W., 2005. Changes in mass and nutrient content of wood during decomposition in a south Florida mangrove forest. J. Ecol. 93, 618–631.
Sariyildiz, T., 2008. Effects of gap-size classes on long-term litter decomposition rates of beech, oak and chest nut species at high elevations in northeast Turkey. Ecosystems 11, 841–853.
Sarjubala Devi, A., Yadava, P.S., 2007. Wood and leaf litter decomposition of *Dipterocarpus tuberculatus* Roxb. in a tropical deciduous forest of Manipur, Northeast India. Curr. Sci. 93, 243–246.
Schaap, M.G., Bouten, W.S., Verstraten, J.M., 1997. Forest floor water content dynamics in a Douglas fir stand. J. Hydrol. 201, 367–383.
Scheu, S., Schauermann, J., 1994. Decomposition of roots and twigs: effects of wood type (beech and ash), diameter, site of exposure and macrofauna exclusion. Plant Soil 163, 13–24.
Schowalter, T.D., Zhang, Y.L., Sabin, T.E., 1998. Decomposition and nutrient dynamics of oak *Quercus* spp. logs after five years of decomposition. Ecography 21, 3–10.
Schultz, T.P., Nicholas, D.D., 2010. Landscape patterns of net nitrification in a northern hardwood-conifer forest. Landscape patterns of net nitrification in a northern hardwood-conifer forest. Wood Fibre Sci. 42, 1–5.
Sonesson, M., Callaghan, T.V., 1991. Strategies of survival in plants of the fennoscandian tundra. Arctic 44, 95–105.
Spano, S.D., Jurgensen, M.F., Larsen, M.J., Harvey, A.E., 1982. Nitrogen-fixing bacteria in Douglas-fir residue decayed by *Fomitopsis pinicola*. Plant Soil 68, 117–123.
Stevens, V., 1997. The Ecological role of coarse woody debris. An overview of the ecological importance of CWD in BC forests. Ministry of Forests Research Program. B.C. Ministry of Forests. Working Paper 30.
Syafii, W., Yoshimoto, T., Samejima, M., 1988. The effect of lignin on decay resistance of some tropical woods. Bull. Tokyo Univ. For. 80, 69–77.
Takyu, M., AIBA, S.I., Kitayama, K., 2003. Changes in biomass, productivity and decomposition along topographical gradients under different geological conditions in tropical lower montane forests on Mount Kinabalu, Borneo. Oecologia 134, 397–404.
Terziev, N., Nilsson, T., 1999. Effect of soluble nutrient content in wood on its susceptibility to soft rot and bacterial attack in ground test. Holzforschung 53, 575–579.
Toledo, J.J., Magnusson, W.E., Castilho, C.V., 2009. Influence of soil, topography and substrates on differences in wood decomposition between one-hectare plots in lowland tropical moist forest in Central Amazonia. J. Trop. Ecol. 25, 649–656.
Torres, J.A., 1994. Wood Decomposition of cyrilla racemiflora in a tropical montane forest. Biotropica 26, 124–140.
Trofymow, J.A., 1998. The Canadian Intersite Decomposition Experiment (CIDET): Project and site establishment report. CIDET Working Group. Nat. Resour. Can., Can. For. Serv., Pac. For. Cent., Victoria, B.C.; Inf. Rep. BC-X-378.
van der Wal, A., de Boer, W., Smant, W., van Veen, J.A., 2007. Initial decay of woody fragments in soil is influenced by size, vertical position, nitrogen availability and soil origin. Plant Soil 301, 189–201.
Venterea, R.T., Lovett, G.M., Groffman, P.M., Schwarz, P.A., 2003. Landscape patterns of net nitrification in a northern hardwood-conifer forest. Soil Sci. Soc. Am. J. 67, 527–539.
Vogt, K.A., Vogt, D.J., Boon, P., Covich, A., Scatena, F.N., Asbjornsen, H., O'Harra, J.L., Perez, J., Siccama, T.G., Bloomfield, J., Ranciato, J.F., 1996. Litter dynamics along stream, riparian and upslope areas following Hurricane Hugo, Luquillo Experimental Forest, Puerto. Biotropica 28, 458–470.
Weedon, J.T., Cornwell, W.K., Cornelissen, J.H.C., Zanne, A.E., Wirth, C., Coomes, D.A., 2009. Global meta-analysis of wood decomposition rates: a role for trait variation among tree species? Ecol. Lett. 12, 45–56.
Zhang, C.F., Meng, F.R., Trofymow, J.A., Arp, P.A., 2007. Modelling mass and nitrogen remaining in litterbags for Canadian forest and climate conditions. Can. J. Soil Sci. 87, 413–432.
Zhang, C.F., Meng, F.-R., Bhatti, J.S., Arp, P.A., 2008. Modeling forest leaf-litter decomposition and N mineralization in litterbags, placed across Canada: a 5-model comparison. Ecol. Model. 219, 342–360.